Applied Catalysis B: Environmental 108–109 (2011) 161–167

Contents lists available at SciVerse ScienceDirect

Applied Catalysis B: Environmental

journal homepage: www.elsevier.com/locate/apcatb

Niobium-containing MCM-41 silica catalysts for biodiesel production

Cristina García-Sancho, Ramón Moreno-Tost, Josefa M. Mérida-Robles, José Santamaría-González, Antonio Jiménez-López, Pedro Maireles-Torres*

Departamento de Química Inorgánica, Cristalografía y Mineralogía (Unidad Asociada al ICP-CSIC), Facultad de Ciencias, Universidad de Málaga, Campus de Teatinos s/n, 29071 Málaga, Spain

ARTICLE INFO

Article history:
Received 19 April 2011
Received in revised form 8 August 2011
Accepted 18 August 2011
Available online 25 August 2011

Keywords:
Niobium oxide
Mesoporous silica
Biodiesel
Transesterification
Acid catalysis

ABSTRACT

This research focuses on the synthesis and characterization of mesoporous niobosilicate molecular sieves and their catalytic activity in biodiesel production by transesterification of sunflower oil with methanol. Catalysts were prepared by two procedures: impregnation of a MCM-41 silica with different amounts of niobium oxalate and subsequent calcination, and structural incorporation of Nb into a MCM-41 silica during the synthesis step. Characterization techniques such as XRD, XPS, TEM, NH_3-TPD and N_2 sorption have been employed to characterize the synthesized catalysts. The biodiesel yield increases with the catalyst acidity, attaining a value of 95% with a 7.5 wt% of a MCM-41 silica impregnated with a 8% of Nb_2O_5, at 200 °C, after 4 h of reaction and a methanol/oil molar ratio of 12. The potential of this family of catalysts to treat low-grade oils has been demonstrated by increasing the acidity of the sunflower oil by adding oleic acid (1.1 wt%) and water (0.2 wt%) to the reaction mixture, since the biodiesel yield is maintained close to 80%. Moreover, the catalyst reutilization has been demonstrated during five catalytic runs by employing a low-grade oil, with no leaching of the active phase.

1. Introduction

The search of new sustainable fuels from renewable resources has attracted considerable attraction in recent years due to the drawbacks of traditional fossil fuels and increasing crude oil prices, as well as the environmental concerns of conventional fuels. In this sense, much attention is nowadays being paid to the production of biodiesel, a biodegradable and renewable fuel, consisting of monoalkyl esters of fatty acids prepared from crude and refined triglyceride containing raw materials, such as vegetable oils, animal fats and wastes. Conventional processes of biodiesel production involve the use of homogeneous alkaline catalysts under mild temperatures (60–80 °C) and atmospheric pressure [1]. However, these catalysts require additional neutralization and separation steps of the final reaction mixture, thus leading to a series of environmental problems related to the use of high amounts of water and energy. Moreover, transesterification reactions can also be performed by using acid catalysts such as sulphuric, sulfonic, phosphoric and hydrochloric acids, under homogeneous conditions. These catalysts have been proposed to promote simultaneous esterification of free fatty acids (FFAs) and transesterification of triglycerides in a single catalytic step [2]. However, acid-catalyzed transesterification has received less attention due to its relatively lower reaction rate in comparison with the base-catalyzed one.

On the other hand, it is known that the production of biodiesel under heterogeneous conditions would result in simpler, cheaper separation processes, a reduced water effluent load, as well as capital and energy costs. However, the replacement of homogeneous catalysts by solid catalysts in transesterification reactions is limited by the need of higher temperature, pressure and methanol to oil molar ratio, as compared with the homogeneous process. The development of solid base catalysts has been widely described in the literature [3]. The use of acid solids to catalyze transesterification reactions is an emerging research field, since recent studies have proved the technical feasibility and the environmental and economical benefits of biodiesel production via heterogeneous acid-catalyzed transesterification [4–6]. In this sense, Melero et al. [7] have reviewed the application of different heterogeneous acid catalysts for biodiesel production, with special attention to the strategies to tune the acid strength and to control the hydrophobic microenvironment of the acid sites, and the subsequent improvements of the catalytic performance. Regarding to inorganic acid catalysts, these authors concluded that there is a whole library of different acid catalysts which can effectively be used for transesterification of vegetable oils. Among them, we can find sulphated metal oxides such as zirconia [8–12], mixed metal oxides [13,14], supported heteropolyacids [15–18], as well as zeolites, heterogenized metal cyanides, vanadyl phosphate [19,20] and many others. Portilho et al. [21] have recently patented the use of Nb_2O_5/H_3PO_4

* Corresponding author. Tel.: +34 952137534; fax: +34 952131870.
E-mail address: maireles@uma.es (P. Maireles-Torres).

0926-3373/$ – see front matter © 2011 Elsevier B.V. All rights reserved.
doi:10.1016/j.apcatb.2011.08.025

system as heterogeneous catalyst for the production of biodiesel from vegetable oils and fats. In fact, niobium oxides and its compounds exhibit a great variety of functions in catalysis, such as promoter, support, redox and acid properties. Thus, niobium containing materials have been proposed as effective catalysts in the dehydration of alcohols, hydrolysis, oxidation, esterification, alkylation, isomerization, and photocatalysis [22–25].

The attachment of niobium oxide over high surface area supports can favour the enhancement of the number of active sites, since the niobium oxide itself exhibits low surface area. Last years have brought the increasing interest in niobium-containing mesoporous molecular sieves. MCM-41 materials are appropriated mesoporous molecular sieves to be used to disperse heteroatoms to generate active sites with acid and/or redox properties. Isomorphous substitution of Si by transition metals has been widely reported in the literature [26–28]. Niobosilicate mesoporous molecular sieves, denoted as Nb/MCM-41, was synthesized for the first time by Ziolek et al. [29,30]. Since then, a significant progress has been made in the preparation of new types of ordered Nb-silica materials [26,31–36]. The different surface species and catalytic performance depend on the metal precursor, metal loading and synthesis conditions. Thus, for low niobium oxide loading (1 wt%) on silica, the resulting materials contain predominantly isolated [NbO_4] units, while Nb cations in supported Nb_2O_5/SiO_2 catalysts form polymerized NbO_x species and/or bulk Nb_2O_5 with increasing Nb loading [37–39]. Moreover, it has been reported that supported niobium oxide on silica exhibit both Brønsted and Lewis acid sites, which remain bound to the support surface even in the presence of water and act as an effective catalyst for acid-catalyzed reactions [40–44].

The present research work deals with the catalytic behaviour of mesoporous niobosilicate molecular sieves in biodiesel production from sunflower oil, under heterogeneous acid-catalyzed conditions. The influence of experimental variables such as reaction temperature and time, and catalyst concentration was investigated. The catalytic results were correlated with the physico-chemical properties of the different catalysts synthesised. Furthermore, the presence of free fatty acids (FFA) and water in the sunflower oil, as well as the reutilization of the catalysts, have been also evaluated.

2. Experimental

2.1. Catalyst preparation

Different niobium-containing mesoporous silica solids have been synthesized by using two methods. Firstly, Nb was structurally incorporated into a mesoporous silica framework according to a procedure similar to that reported by Ziolek et al. [29]: 8.23 g of sodium silicate (26.5% SiO_2 in 14% NaOH) was stirred with 50 g of distilled water for 10 min, then 28.12 g of a template/water mixture (cetyltrimethylammonium bromide, 25 wt% solution in water) and a niobium oxalate solution (1.46 g of niobium oxalate in 10.89 g of 0.1 M oxalic acid) were added. The formed gel with a Si/Nb molar ratio of 16.2 was stirred at room temperature for 7 days. The solid product was filtrated, washed with distilled water and dried in air at 60 °C. The template was removed by calcination at 550 °C during 6 h. This material was denoted as Nb-MCM.

Another family of materials was prepared by incipient wetness impregnation of a MCM-41 silica, prepared as previously described [45]. The impregnation was carried out by using an aqueous solution of niobium oxalate in 0.1 M oxalic acid to obtain Nb_2O_5 weight percentages in the resulting catalysts of 3, 5, 8 and 16. After impregnation, materials were dried in air at 60 °C and calcined at 550 °C during 6 h. These materials were denoted as MCM-Nb*x*, where *x* indicates the wt% of Nb_2O_5 incorporated to the MCM-41 materials.

2.2. Catalyst characterization

Elemental analysis was performed on a PERKIN-ELMER 2400 CHN with a LECO VTF900 pyrolysis oven. Nb content has been determined by ICP-AES by using a Perkin Elmer (model ELAN DRC-e) spectrometer.

Powder XRD patterns were obtained by using a Siemens D5000 automated diffractometer, over a 2θ range with Bragg–Brentano geometry using the Cu Kα radiation and a graphite monochromator. Transmission electron micrographs (TEM) of the samples were obtained by using a Philips CM 200 Supertwin-DX4 microscope. Samples were dispersed in ethanol, and a drop of the suspension was put on a Cu grid (300 mesh).

X-ray photoelectron spectroscopy (XPS) studies were performed with a Physical Electronics PHI 5700 spectrometer equipped with a hemispherical electron analyzer (model 80-365B) and a Mg Kα (1253.6 eV) X-ray source. High-resolution spectra were recorded at 45° take-off-angle by a concentric hemispherical analyzer operating in the constant pass energy mode at 29.35 eV, using a 720 mm diameter analysis area. Charge referencing was done against adventitious carbon (C 1s at 284.8 eV). The pressure in the analysis chamber was kept lower than 5×10^{-6} Pa. PHI ACCESS ESCA-V6.0 F software package was used for data acquisition and analysis. A Shirley-type background was subtracted from the signals. Recorded spectra were always fitted using Gauss–Lorentz curves in order to determine more accurately the binding energy of the different element core levels.

N_2 adsorption–desorption isotherm at −196 °C was obtained using an ASAP 2020 model of gas adsorption analyzer from Micromeritics, Inc. Prior to N_2 adsorption, the sample were evacuated at 200 °C (heating rate 10 °C min^{-1}) for 10 h. Pore size distributions and pore volume were calculated with the BJH method.

Temperature-programmed desorption of ammonia (NH_3-TPD) was carried out to evaluate the total acidity of the catalysts. After cleaning the materials with helium and adsorption of ammonia at 100 °C, the NH_3-TPD was performed between 100 and 550 °C with a heating rate of 10 °C min^{-1} by using a helium flow and maintained at 550 °C for 15 min. The evolved ammonia was analyzed by on-line gas chromatography (Shimadzu GC-14A) provided with a TCD.

2.3. Catalytic tests

The methanolysis of edible sunflower oil was performed at 200 °C by using a Parr high pressure reactor with 100 mL capacity and a stirring rate of 300 rpm. Catalysts were used without activation. In a typical experiment, 10 g of oil was incorporated to the reactor together with the methanol and different amount of catalyst. The methanol/oil molar ratio was 12. After reaction, the system was cooled and then an aliquot (2 mL) was taken and treated with 1 mL of distilled water and shaking for few minutes. Later, 1 mL of dichloromethane was added, and this mixture was again agitated and set aside to develop two phases: the non-polar phase containing dichloromethane, mono-, di- and triglycerides and methyl esters of fatty acids (FAME) (and traces of methanol and glycerol) and the polar phase containing water, glycerol and methanol (and traces of esters). The dichloromethane was then removed from the organic phase by evaporation at 90 °C. The resulting solution was analyzed by high performance liquid chromatography (HPLC) using a JASCO liquid chromatograph equipped with quaternary gradient pump (PU-2089), multiwavelength detector (MD-2015), autosampler (AS-2055), column oven (co-2065) using a PHENOMENEX LUNA C18 reversed-phase column (250 mm × 4.6 mm, 5 μm). The solvents were filtered through a 0.45 μm filter prior use and degassed with helium. A linear gradient from 100% methanol to 50% methanol + 50% 2-propanol/hexane

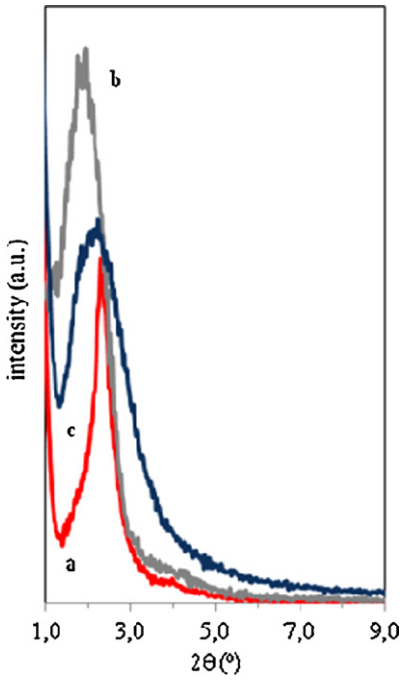

Fig. 1. XRD patterns of Nb-MCM (a), MCM-41 (b) and MCM-Nb8 (c).

(5:4, v/v) in 35 min was employed. Injection volumes of 15 μL and a flow of rate of 1 mL min^{-1} were used. The column temperature was held constant at 40 °C. All samples were dissolved in 2-propanol-hexane (5:4, v/v). The weight content in FAME determined by HPLC was considered to represent the FAME yield (in wt%) of the catalytic process, assuming that, during the neutralization and washing steps of the ester phase, only traces of esters were transferred to the polar phase and that the extraction of methanol and glycerol only takes place.

3. Results and discussion

3.1. Characterization of materials

The X-ray diffraction technique reveals that, after calcination at 550 °C, all the materials exhibit in their XRD patterns the intense and broad low-angle peak characteristic of the hexagonal structure of mesoporous materials (Fig. 1), assigned to the (1 0 0) diffraction line. The absence of other well-defined diffraction peaks in the region $2\theta = 3–8°$ can be justified by the low temperature used in the synthesis of these mesoporous materials, differently from those reported in most of papers, which are synthesized under hydrothermal conditions at higher temperatures. However, the d_{100} peak (3.8 nm) of the Nb-MCM material is narrower, pointing to that incorporation of Nb into the siliceous structure ameliorates the crystallinity of the resulting mesoporous material. The impregnation method gives rise to solids where the d_{100} signal is still observed (for instance, d_{100} = 4.4 nm for the MCM-Nb8 sample), even for high Nb_2O_5 loading, being consistent with data already reported in literature [29], and indicating that the long-range order of the hexagonal mesostructure of the parent MCM-41 silica is preserved after niobium incorporation. XRD patterns in the high-angle region did not evidence the characteristic reflections of crystalline Nb_2O_5 phases, thus pointing to the existence of amorphous or Nb species of small size on the silica surface. Braga et al. [39] have demonstrated the need of increasing the calcination temperature up to 800 °C to form crystalline phases of supported Nb_2O_5.

The absence of large niobium oxide particles which could block the entrance of mesopores was confirmed by nitrogen sorption at −196 °C. The adsorption–desorption isotherms of all synthesized materials are of type IV according to the IUPAC classification (not shown). All of them exhibit the sharp capillary condensation step at relative pressures of 0.3–0.4. Moreover, it is observed an unimodal pore size distribution, typical of mesoporous materials. Their high specific surface areas, pore volumes and pore sizes reveal the mesoporous nature of this family of niobium-containing silica (Table 1). The niobosilicate obtained by structural incorporation (Nb-MCM) shows better textural properties than those obtained by the impregnation method, which is in agreement with the higher structural ordering observed by XRD. The BET surface areas and pore volumes decrease with the Nb loading. Thus, the MCM-41 support has a S_{BET} of 1000 $m^2 g^{-1}$, which is reduced until 880 $m^2 g^{-1}$ after incorporation of a 16% of Nb_2O_5. This reduction can be justified by the increase of the sample density after the incorporation of Nb species, homogeneously dispersed into the mesoporous framework. This behaviour is expected by considering that the highest Nb loading is still lower than that necessary to obtain a complete coverage of the silica surface, which corresponds to a surface density of Nb atoms on silica of $\delta = 2.2$ atoms nm^{-2} [46]. Moreover, the average pore diameters barely change, thus corroborating that Nb_2O_5 particles do not block the mesopores of the MCM-41 support.

Table 1
Textural data and acidic properties.

Catalyst	BET surface area ($m^2 g^{-1}$)	Pore volume ($cm^3 g^{-1}$)	Av. pore diameter (nm)	μmoles NH_3 m^{-2}
Nb-MCM	1211	1.10	2.8	1.16
MCM-41	1000	0.80	2.5	0.13
MCM-Nb3	978	0.76	2.4	1.04
MCM-Nb5	945	0.75	2.5	1.07
MCM-Nb8	891	0.69	2.4	1.29
MCM-Nb16	880	0.68	2.4	0.95

The TEM pictures confirm the well-organized hexagonal pore system of the samples. It was possible to observe the typical hexagonal pore arrangement of MCM-41 type materials (Fig. 2) for both series of mesoporous niobosilicates, Nb-MCM and MCM-Nb*x* materials, although the ordering is higher when Nb is incorporated into the siliceous structure during the synthesis step (Nb-MCM).

X-ray photoelectron spectroscopy is a powerful tool to get insights into the surface nature of solids. The XPS data are summarized in Table 2. The Si 2p signal is symmetrical and appears at binding energy (BE) values of 103.2–103.8 eV, typical of Si in silica. The O 1 s region only shows a single and almost symmetric peak at BE: 532.6–533.0 eV, close to the value observed for a MCM-41 silica (533.0 eV), whereas bulk Nb_2O_5 displays this peak at lower BE (530.2 eV). This confirms again the absence of segregated Nb_2O_5 particles on the external surface of the siliceous support, as can be also deduced from the highest surface Si/Nb molar ratio in comparison with the corresponding bulk values obtained by the XRF technique (Table 2). On the other hand, the two components of the Nb 3d doublet can be well resolved at 207.5–208.1 eV ($3d_{5/2}$) and 210.1–210.9 eV ($3d_{3/2}$), which are typical BE values of Nb(V) in an oxidic environment. Relevant differences were not found in the values of the Si 2p, O 1s and Nb 3d binding energies by varying the Nb loading.

It is well known that the activity in the transesterification reaction depends on the strength of acid and base sites of solid catalysts. For this reason, the total acidity of the synthesised materials was evaluated by NH_3-TPD, in order to confirm the results previously obtained with other members of the MCM-41 family, where the incorporation of heteroatoms, such as aluminum or zirconium, enhances the acidity of the inorganic framework [47]. Thus, the acidity increases from 0.13 (MCM-41 silica) to more than 1.2 μmol NH_3 m^{-2} after the incorporation of Nb (Table 1), and with the Nb content from 1.04 (MCM-Nb3) to 1.29 μmoles NH_3 g^{-1}

Table 2
XPS data (binding energies and Si/Nb atomic ratio) of synthesized catalysts.

Catalyst	Si 2p (eV)	O 1s (eV)	Nb 3d (eV)		Surface Si/Nb atomic ratio	Bulk Si/Nb atomic ratio[a]
Nb-MCM	103.6	533.0	208.1 ($3d_{5/2}$)	210.9 ($3d_{3/2}$)	32.2	10.0
MCM-41	103.8	533.0	–	–	–	–
MCM-Nb3	103.7	533.0	208.0	210.6	85.9	37.5
MCM-Nb5	103.4	532.7	207.5	210.1	55.8	20.8
MCM-Nb8	103.6	533.0	208.0	210.6	51.2	11.7
MCM-Nb16	103.8	533.1	207.9	210.5	41.5	5.5
Nb_2O_5	–	530.2	208.0	210.6	–	–

[a] As determined by X-ray fluorescence.

(MCM-Nb8), revealing a good dispersion of the Nb_2O_5 phase even for the material with the highest Nb content. However, by comparing materials with similar Nb loading obtained by the two methods used in the present work (Nb-MCM and MCM-Nb8), very similar total acidity values are found. Moreover, the temperature range in which ammonia is desorbed gives information about the strength of the acid sites. The integration of the NH_3-TPD curves reveals the presence of acid centers with a wide range of strength. It has been reported that highly distorted NbO_6 octahedra sites correspond to the Lewis acid sites, whereas slightly distorted octahedral as well as NbO_7 and NbO_8 sites are associated to Brönsted acid sites [40]. Both types of acid sites have been detected in niobia supported on silica, and their activity in 2-propanol dehydration to propene was demonstrated [30]. The presence of distorted NbO_6 octahedra has been confirmed by Raman spectroscopy. It is well known that regular tetrahedral NbO_4 structures are associated to Raman frequencies in the 790–830 cm^{-1} region, distorted octahedral NbO_6 structures to values in the 500–700 cm^{-1} region and highly distorted octahedral NbO_6 structures give rise to bands in the 850–1000 cm^{-1} region. The Raman spectra of the MCM-Nb*x* catalysts, under ambient conditions, only show bands associated to Nb species for the highest loading. Thus, the spectrum of the MCM-Nb16 catalyst displays a very broad band extending from 550 to 750 cm^{-1}, which can be assigned to distorted NbO_6 octahedra, similar to that observed for the bulk Nb_2O_5. Therefore, this Raman band could reveal the presence of small Nb_2O_5 particles, not detected by XRD, on the surface of this catalyst, that decreasing the number of acid sites in comparison with the catalyst with a lower Nb_2O_5 loading, MCM-Nb8.

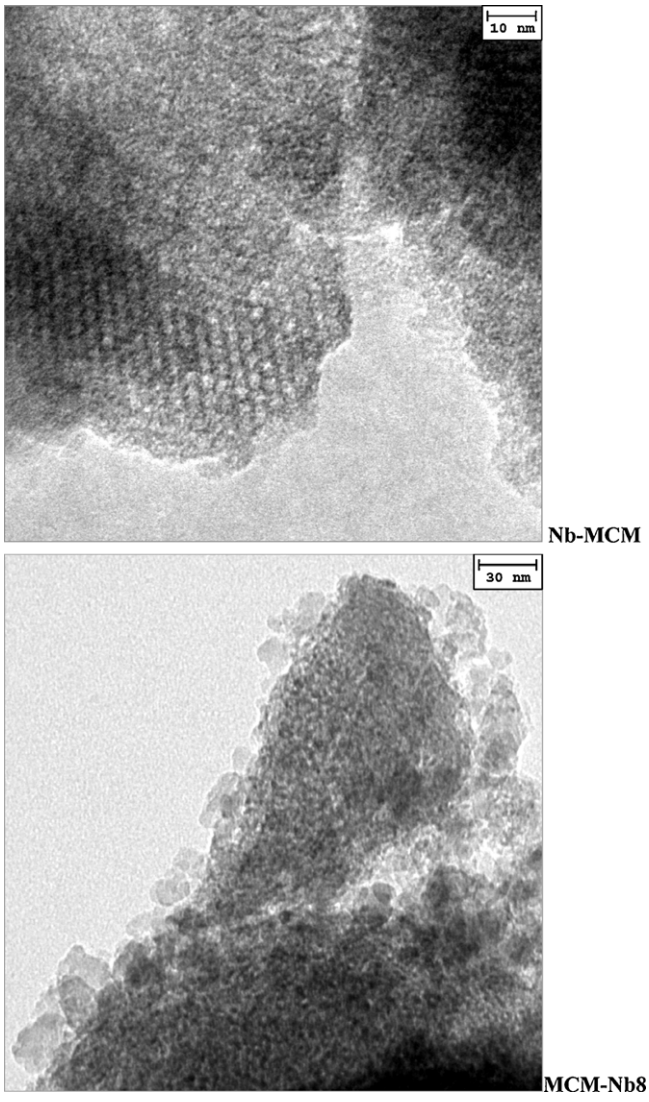

Fig. 2. TEM images of the Nb-MCM and MCM-Nb8 catalysts.

3.2. Catalytic activity

The catalytic activity of these niobium-based catalysts has been evaluated in the transesterification of sunflower oil with methanol, under heterogeneous conditions. The effect of temperature and time of reaction, catalyst concentration and presence of free fatty acids (FFA) and water, on biodiesel conversion have been evaluated. Other parameters, such as stirring rate (300 rpm) and methanol/oil molar ratio (12/1), were maintained constant in all experiments. This methanol/oil molar ratio, exceeding the stoichiometric value, was used to favour the biodiesel formation [48].

Firstly, it was carried out a study by using different temperature and reaction time values. The influence of these two parameters was evaluated for both the non-catalytic process (in the absence of catalyst) and the heterogeneous process catalyzed by the MCM-Nb8 catalyst. In these studies, a catalyst loading of 5 wt% respect to the oil weight and a reaction time of 6 h were employed. The conversion to biodiesel becomes important for the heterogeneous process at 200 °C (Fig. 3), when a biodiesel yield close to 90% is obtained; however, at this temperature, there is also a contribution of the non-catalytic process of 42%. However, by decreasing the reaction time to 4 h, this non-catalytic contribution is reduced until 24%, whereas the overall biodiesel yield is still of 81% (Fig. 4). Therefore, a temperature of 200 °C and a time of reaction of 4 h were chosen.

A catalytic screening of all niobium-based catalysts has been carried out under the following experimental conditions: reaction temperature of 200 °C, 4 h of reaction and 5 wt% of catalyst respect to the oil. As observed in Fig. 5, the pure mesoporous MCM-41 silica is not active due to its very weak acidity; in fact, its catalytic behaviour is similar to that observed in the non-catalytic process. Among the impregnated niobium catalysts (MCM-Nb*x*), the biodiesel yield increases with the Nb_2O_5 loading from 3 to 8 wt%, achieving a value of 87% for the MCM-Nb8

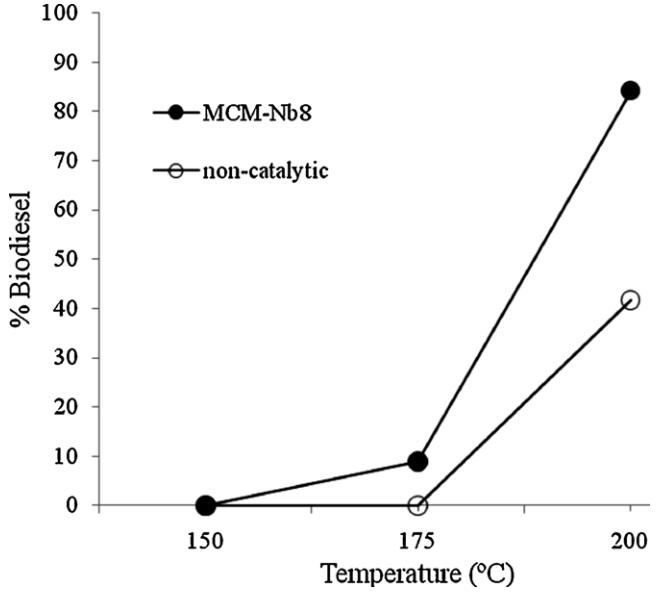

Fig. 3. Evolution of the biodiesel yield in the methanolysis of sunflower oil of the MCM-Nb8 catalyst and the non-catalytic process as a function of the reaction temperature (reaction conditions: methanol/oil molar ratio = 12, catalyst = 5 wt%, stirring rate = 300 rpm, time = 6 h).

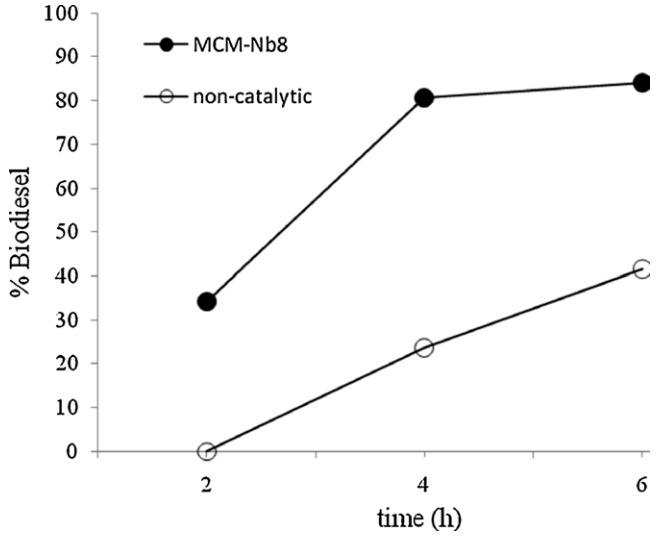

Fig. 4. Influence of the reaction time on the transesterification of sunflower oil with methanol over the MCM-Nb8 catalyst (reaction conditions: catalyst = 5 wt%, stirring rate = 300 rpm, T = 200 °C, methanol/oil molar ratio = 12).

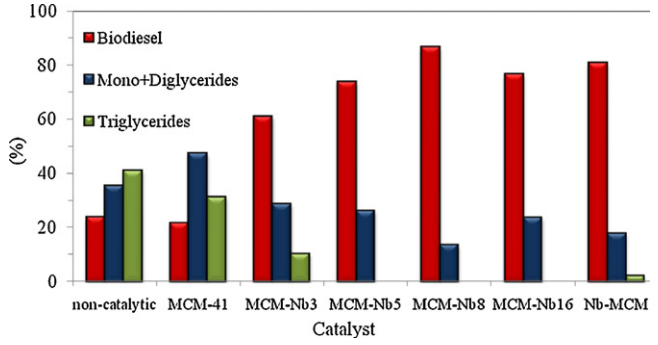

Fig. 5. Biodiesel yield over the different mesoporous niobosilicates (reaction conditions: methanol/oil molar ratio = 12, stirring rate = 300 rpm, T = 200 °C, reaction time = 4 h, catalyst weight = 5 wt%).

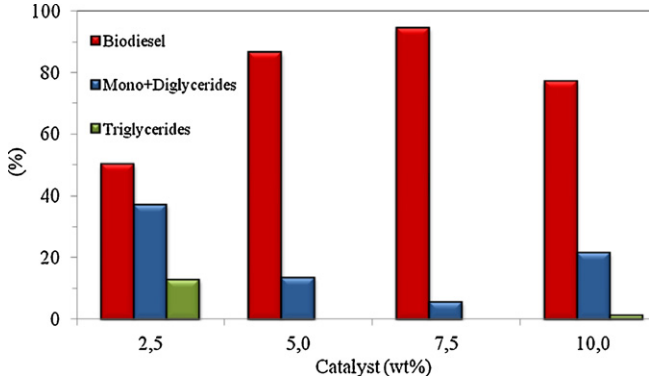

Fig. 6. Influence of the catalyst weight on the biodiesel yield over the MCM-Nb8 catalyst (reaction conditions: methanol/oil molar ratio = 12, stirring rate = 300 rpm, T = 200 °C, reaction time = 4 h).

catalyst. The biodiesel yield slightly decreases for higher loading. Full triglycerides conversion is observed over all impregnated catalysts, excepting the catalyst with the lowest niobium content (MCM-Nb3). Thus, the conversion to mono- and diglycerides decreases and that to biodiesel increases when the Nb_2O_5 loading goes from 3 to 8%. This evolution of the catalytic performance in biodiesel production is in agreement with the acid properties of this family of supported niobium catalysts, since by NH_3-TPD was demonstrated that MCM-Nb8 exhibits the highest acidity. The catalytic behaviour of the Nb-MCM catalyst is similar, although a total conversion of triglyceride is not achieved.

It is well known that catalyst concentration affects the yield in biodiesel production. The effect of this parameter was studied at 200 °C after 4 h of reaction, by using the MCM-Nb8 catalyst. For the lowest catalyst concentration (2.5 wt%), the total conversion of triglycerides was not achieved, whereas a high conversion to mono- and diglycerides is observed (Fig. 6). As can be expected, by increasing the catalyst concentration from 2.5 to 7.5 wt%, the biodiesel yield increases markedly from 50 to 95% (Fig. 6). However, the catalytic activity is not ameliorated by a further increase of the catalyst loading, probably due to mass transfer limitations because the stirring rate and the total volume of reactants were maintained unchanged, and the amount of catalyst is too high to achieve a suitable contact with reactants.

On the other hand, the reduction of biodiesel production costs can be achieved by using low-cost feedstocks, such as used frying oils and animal fats with a high content of water and FFAs. The processing of these low-cost raw materials poses a challenge in the production of second generation biofuels by using the conventional base-catalyzed homogeneous process. In this sense, the development of solid acid catalysts which can be able to simultaneously carry out the esterification of FFAs and transesterification of triglycerides, under heterogeneous conditions, is an interesting alternative for the treatment of these feedstocks. In this work, simulated used frying oils have been prepared by adding different amounts of oleic acid and water to a sunflower oil. Fig. 7 displays the results of this study carried out at 200 °C, after 4 h of reaction, and using a 5 wt% of the MCM-Nb8 catalyst. As it has been previously demonstrated, with an edible sunflower oil (0.2 wt% of acidity, defined as g of oleic acid per 100 g of oil), a total conversion of triglycerides with a 87% of biodiesel yield can be achieved. However, in the presence of a 0.2 wt% of water, the biodiesel production slightly decreases until 81%, although the conversion of triglycerides is also complete. By increasing this acidity until 1.1 wt%, with a 0.2 wt% of water, the conversion and selectivity values were not affected. Nevertheless, a further increasing in water content (0.4 wt%) to the oil with a 1.1 wt% of acidity gives rise to an important decrease of biodiesel production (from 80 to 67%). However, if

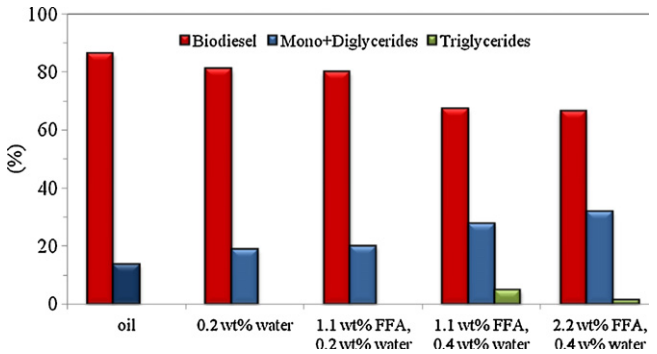

Fig. 7. Influence of the addition of oleic acid (FFA) and water to the sunflower oil on the biodiesel yield over the MCM-Nb8 catalyst (reaction conditions: methanol/oil molar ratio = 12, stirring rate = 300 rpm, T = 200 °C, reaction time = 4 h, catalyst weight = 5 wt%).

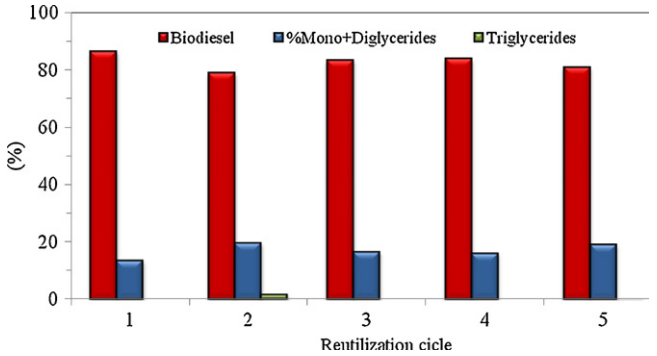

Fig. 8. Study of the reutilization of the MCM-Nb8 catalyst (reaction conditions: methanol/oil molar ratio = 12, stirring rate = 300 rpm, T = 200 °C, reaction time = 4 h, catalyst weight = 5 wt%, acidity = 1.1 wt%, water content = 0.2 wt%).

the acidity of this oil with a 0.4 wt% of water is again increased to 2.2 wt%, the production of biodiesel is practically maintained. From this study, it can be concluded that the presence of water exerts a negative effect on the biodiesel production, although this was higher than 60% after the addition of 0.4 wt% of water. On the other hand, the addition of FFA until 2.2 wt% has not an appreciable effect on the catalytic performance under the experimental conditions used in this study.

Another key aspect in the development of new solid catalysts for biodiesel production, under heterogeneous conditions, is the possibility of reutilization of the solid catalyst. For this study, the catalyst was recovered after each run by decantation and put on contact with a new reaction mixture, but containing 0.2 wt% of water and an acidity degree of 1.1 wt%. The catalytic results reveal that the MCM-Nb8 catalyst maintains its activity after five catalytic runs (Fig. 8), revealing that this solid acid catalyst can be reused, without activation, to process low quality oils. After the fifth catalytic run, the biodiesel yield is still close to 80%. After each catalytic run, the acidity degree, as determined by titration with KOH, was lower than 0.1 mg KOH/g biodiesel. This result is expected since the MCM-Nb8 catalyst accomplishes the full esterification of oleic acid with methanol, under similar experimental conditions (T = 200 °C, methanol/oleic acid molar ratio of 12, 5 wt% of catalyst and 4 h of reaction time). Moreover, the leaching of Nb from the solid catalyst to the liquid medium can be ruled out since the presence of Nb in solution was not detected, and the surface Si/Nb molar ratio in the spent catalyst (52.2) was similar to that in the fresh one (51.2).

Therefore, by comparing the catalytic behaviour in biodiesel production of the niobium-containing silica catalysts described in the present work with other solid acid catalysts reported in literature, it can be inferred that, although the former require a relatively high reaction temperature (200 °C), the rest of experimental variables (reaction time, methanol/oil molar ratio, catalyst loading and reutilization potential even in the presence of FFA) are very favourable to find industrial application. In literature, more drastic experimental conditions (higher reaction times and temperatures, as well as methanol/oil molar ratios) can be found for solid acid catalysts [7,13], and, in some cases, although they exhibit a better performance under moderate experimental conditions, deactivation is observed [9]. However, it is evident that solid base catalysts do work at a much lower temperature and shorter reaction time, but they suffer from neutralization in the presence of FFA, which limits their use for treating low-cost feedstocks.

4. Conclusions

Biodiesel production can be achieved via methanolysis of sunflower oil catalyzed by mesoporous niobosilicates. Niobium species are dispersed on the silica surface, generating acid sites able to simultaneously catalyze the esterification of oleic acid and the transesterification of sunflower oil, even in the presence of a 0.2 wt% of water. The catalytic activity is related to the acidity of the catalysts, as determined by NH_3-TPD, attaining a biodiesel yield of 95% by using a 7.5 wt% of a MCM-41 silica impregnated with a 8% of Nb_2O_5, at a reaction temperature of 200 °C, after 4 h of reaction and a methanol/oil molar ratio of 12. The potential of this family of catalysts to treat low-grade oils has been demonstrated by increasing the acidity of the sunflower oil with oleic acid (1.1 wt%) and by adding water (0.2 wt%) to the reaction mixture, since the biodiesel yield is maintained close to 80%. Moreover, this family of catalysts can be reutilised, without activation, at least during five catalytic runs, maintaining biodiesel yields close to 70% even in the presence of oleic acid (2.2 wt%) and water (0.4 wt%), without leaching of the active phase.

Acknowledgements

The authors are grateful to the Spanish Ministry of Science and Innovation (ENE2009-12743-C04-03 project) and Junta de Andalucía (P09-FQM-5070) for financial support. RMT would like to thank this Ministry of Science and Innovation for the financial support under the Program Ramón y Cajal (RYC-2008-03387).

References

[1] F.R. Ma, M.A. Hanna, Bioresour. Technol. 70 (1999) 1–15.
[2] E. Lotero, Y. Liu, D.E. Lopez, K. Suwannakaran, D.A. Bruce, J.G. Goodwin Jr., Ind. Eng. Chem. Res. 44 (2005) 5353–5363.
[3] M. Di Serio, R. Tesser, L. Pengmei, E. Santacesaria, Energy Fuels 22 (2008) 207–217.
[4] A.H. West, D. Posarac, N. Ellis, Bioresour. Technol. 99 (2008) 6587–6601.
[5] J.M. Marchetti, V.U. Miguel, A.F. Errazu, Fuel Process. Technol. 89 (2009) 740–748.
[6] M. Hara, ChemSusChem 2 (2009) 129–135.
[7] J.A. Melero, J. Iglesias, G. Morales, Green Chem. 11 (2009) 1285–1308.
[8] J. Jitputti, B. Kitiyanan, P. Rangsunvigit, K. Bunyakiat, L. Attanatho, P. Jenvanitpanjakul, Chem. Eng. J. 116 (2006) 61–66.
[9] C. Martins-Garcia, S. Teixeira, L. Ledo Marciniuk, U. Schuchardt, Bioresour. Technol. 99 (2008) 6608–6613.
[10] D.E. López, J.G. Goodwin Jr., D.A. Bruce, S. Furuta, Appl. Catal. A 339 (2008) 76–83.
[11] K. Suwannakarn, E. Lotero, K. Ngaosuwan, J.G. Goodwin Jr., Ind. Eng. Chem. Res. 48 (2009) 2810–2818.
[12] B. Fu, L. Gao, L. Niu, R. Wei, G. Xiao, Energy Fuels 23 (2009) 569–572.
[13] S. Furuta, H. Matsuhashi, K. Arata, Catal. Commun. 5 (2004) 721–723.
[14] S. Furuta, H. Matsuhashi, K. Arata, Biomass Bioenergy 30 (2006) 870–873.
[15] M.G. Kulkarni, R. Gopinath, L.C. Meher, A.K. Dalai, Green Chem. 8 (2006) 1056–1062.
[16] F. Chai, F. Cao, F. Zhai, Y. Chen, X. Wang, Z. Su, Adv. Synth. Catal. 349 (2007) 1057–1065.
[17] F. Cao, Y. Chen, F. Zhai, J. Li, J. Wang, X. Wang, S. Wang, W. Zhu, Biotechnol. Bioeng. 101 (2008) 93–100.
[18] L. Xu, Y. Wang, X. Yang, X. Yu, Y. Guo, J.H. Clark, Green Chem. 10 (2008) 746–755.

[19] M. Di Serio, M. Cozzolino, R. Tesser, P. Patrono, F. Pinzari, B. Bonelli, E. Santacesaria, Appl. Catal. A 320 (2007) 1–7.
[20] E. Santacesaria, G. Minutillo, M. Di Serio, P. Patrono, F. Pinzari, M. Ledda, R. Tesser, D. Siano, WO Pat. 062825 A1 (2007).
[21] M.F. Portilho, J.A. V. Vieira, J.L. Zotin, M.S.S. Lima, US Pat. 0295393 A1 (2008).
[22] I. Nowak, M. Ziolek, Chem. Rev. 99 (1999) 3603–3624.
[23] K. Tanabe, Catal. Today 78 (2003) 65–77.
[24] M. Ziolek, Catal. Today 78 (2003) 47–64.
[25] K. Tanabe, S. Okazaki, Appl. Catal. A 133 (1995) 191–218.
[26] V. Parvulescu, C. Anastasescu, C. Constantin, B.L. Su, Catal. Today 78 (2003) 477–485.
[27] V. Parvulescu, C. Anastasescu, B.L. Su, J. Mol. Catal. A 211 (2004) 143–148.
[28] A. Corma, H. Garcia, Chem. Rev. 102 (2002) 3837–3892.
[29] M. Ziolek, I. Nowak, Zeolites 18 (1997) 356–360.
[30] M. Ziolek, I. Nowak, J.C. Lavalley, Catal. Lett. 45 (1997) 259–265.
[31] K. Schumacher, M. Grun, K.K. Unger, Micropor. Mesopor. Mater. 27 (1999) 201–206.
[32] I. Nowak, Stud. Surf. Sci. Catal. 142 (2002) 1363–1370.
[33] X.T. Gao, I.E. Wachs, M.S. Wong, J.Y. Ying, J. Catal. 203 (2001) 18–24.
[34] I. Nowak, Colloids Surf. A: Physicochem. Eng. Aspects 241 (2004) 103–111.
[35] J.M.R. Gallo, H.O. Pastore, U. Schuchardt, J. Non-Cryst. Solids 354 (2008) 1648–1653.
[36] S. Sumiya, Y. Oumi, M. Sadakane, T. Sano, Appl. Catal. A 365 (2009) 261–267.
[37] N. Ichikuni, M. Shirai, Y. Iwasawa, Catal. Today 28 (1996) 49–58.
[38] X. Gao, I.E. Wachs, M.S. Wong, J.Y. Ying, J. Catal. 203 (2001) 18–24.
[39] V.S. Braga, J.A. Dias, S.C.L. Dias, J.L. de Macedo, Chem. Mater. 17 (2005) 690–695.
[40] J.M. Jehng, I.E. Wachs, Catal. Today 8 (1990) 37–55.
[41] J.M. Jehng, I.E. Wachs, J. Mol. Catal. 67 (1991) 369–387.
[42] M. Shirai, N. Ichikuni, K. Asakura, Y. Iwasawa, Catal. Today 8 (1990) 57–66.
[43] N.K. Mal, A. Bhaumik, P. Kumar, M. Fujiwara, Chem. Commun. 9 (2003) 872–873.
[44] N.K. Mal, A. Bhaumik, M. Fujiwara, M. Matsukata, Micropor. Mesopor. Mater. 93 (2006) 40–45.
[45] A. Infantes-Molina, J. Mérida-Robles, P. Braos-García, E. Rodríguez-Castellón, E. Finocchio, G. Busca, P. Maireles-Torres, A. Jiménez-López, J. Catal. 225 (2004) 479–488.
[46] J.G. Weissman, E.I. Ko, P. Wijnblatt, J. Catal. 108 (1987) 383–400.
[47] D. Fuentes-Perujo, J. Santamaría-González, J. Mérida-Robles, E. Rodríguez-Castellón, A. Jiménez-López, P. Maireles-Torres, R. Moreno-Tost, R. Mariscal, J. Solid State Chem. 179 (2006) 2182–2189.
[48] D.Y.C. Leung, X. Wu, M.K.H. Leung, Appl. Energy 87 (2010) 1083–1095.